

# Colorimetric sensing of Cu(II) by 2-methyl-3-[(pyridin-2-ylmethyl)-amino]-1,4-naphthoquinone: Cu(II) induced deprotonation of NH responsible for color changes†

Shu-Pao Wu,\* Ray-Yui Huang and Kun-Ju Du

Received 16th December 2008, Accepted 1st April 2009

First published as an Advance Article on the web 29th April 2009

DOI: 10.1039/b822613j

1,4-Naphthoquinone based chemosensors **1** and **2** detect only the presence of Cu<sup>2+</sup> ions among other transition metal ions by changing color from orange to dark blue. Chemosensors **1** and **2** function as tridentate ligands, which bind Cu<sup>2+</sup> ions through three functional groups: an amine nitrogen, a pyridine nitrogen and a quinone oxygen. On addition of Cu<sup>2+</sup>, both **1** and **2** exhibit a 168 nm red shift in absorption wavelength (pH 7.0). The effect on pH by the formation of these Cu<sup>2+</sup> complexes was determined by UV-vis spectroscopic pH titration. In the pH range of 6–7.5, a maximum was observed at 634 nm and exhibited the formation of deprotonated **1**-Cu<sup>2+</sup> and **2**-Cu<sup>2+</sup> complexes. A reversible color change (orange–blue–orange) was observed when chemosensor **1** was mixed with Cu<sup>2+</sup> in CH<sub>3</sub>CN. This represents a reversible process of deprotonation and re-protonation of the **1**-Cu<sup>2+</sup> complexes and also demonstrates the short half-life of the deprotonated **1**-Cu<sup>2+</sup> complexes in CH<sub>3</sub>CN.

## Introduction

In recent years, an intense effort has been placed on the development of molecular devices for Cu<sup>2+</sup> detection.<sup>1</sup> Copper is the third most abundant essential transition metal ion in the human body and plays important physiological roles in many biological systems.<sup>2,3</sup> Copper ions can react with molecular oxygen to form reactive oxygen species (ROS), which can damage proteins, nucleic acids and lipids. The cellular toxicity of copper ions is connected to serious neurodegenerative diseases, including Menkes and Wilson disease<sup>4,5</sup>, Alzheimer's disease,<sup>6</sup> and prion disease.<sup>7</sup> Due to the extensive use of copper in modern society, Cu<sup>2+</sup> is a significant metal pollutant. In order to better detect and monitor the presence of Cu<sup>2+</sup> ions, the demand for sensitive and selective Cu<sup>2+</sup> chemosensors has garnered much attention.

Cu<sup>2+</sup> recognition is a key issue for the design of Cu<sup>2+</sup> chemosensors. Cu<sup>2+</sup> can induce deprotonation of NH groups conjugated to aromatic compounds or in amide bonds upon Cu<sup>2+</sup> binding. This deprotonation process caused by Cu<sup>2+</sup> binding can be used for Cu<sup>2+</sup> recognition. Peptides such as gly-gly-his<sup>1b,1d</sup> and gly-his<sup>1c</sup> can selectively bind Cu<sup>2+</sup> to deprotonated amides and have been developed for Cu<sup>2+</sup> sensing. In addition, Cu<sup>2+</sup> induced deprotonation of NH groups conjugated to aromatic compounds such as anthrance-9,10-dione<sup>1a,1j</sup> and naphthalimide<sup>1g</sup> cause an internal charge transfer (ICT), which can be observed as a shift in absorption wavelength. This mechanism is responsible for the color change (*i.e.* shift in absorption wavelength) and has been

recently demonstrated as an excellent way for highly selective Cu<sup>2+</sup> detection.

Similarly, anion induced polarization/deprotonation of NH on anilides and aryl urea has been used for anion sensing.<sup>8</sup> Anions form hydrogen bonds with the proton in the NH group and yield a partial negative charge in the amine. In extreme cases, the proton in the NH group is removed to yield a negative charge in the amine. Anion induced polarization/deprotonation of NH on anilides and aryl urea causes an internal charge transfer (ICT), which can be observed as a shift in absorption wavelength. In contrast, in the process of Cu<sup>2+</sup> induced deprotonation of NH, Cu<sup>2+</sup> binds to the amine through an interaction with the lone-pair electrons and thus induces deprotonation of NH. The color change caused by Cu<sup>2+</sup> induced deprotonation of NH is not simply due to deprotonation by Cu<sup>2+</sup>, because Cu<sup>2+</sup> can also influence the electronic state of the chromophore.

In this work, 2-methyl-1,4-naphthoquinone based chemosensors were utilized for Cu<sup>2+</sup> detection. 2-Methyl-1,4-naphthoquinone (menadione) belongs to the vitamin K family (vitamin K3) and many 1,4-naphthoquinone derivatives display notable antibacterial activities.<sup>9</sup> The 2-methyl-1,4-naphthoquinone based chemosensors were constructed by the linkage of 2-methyl-1,4-naphthoquinone with two bidentate ligands, 2-(aminomethyl)pyridine and 2-(aminoethyl)pyridine, *via* an amine group (Fig. 1). Several anions (CN<sup>-</sup>, F<sup>-</sup>, Cl<sup>-</sup>, Br<sup>-</sup>, H<sub>2</sub>PO<sub>4</sub><sup>-</sup>, HSO<sub>4</sub><sup>-</sup>, NO<sub>3</sub><sup>-</sup>, ClO<sub>4</sub><sup>-</sup>, CO<sub>3</sub><sup>2-</sup>, OH<sup>-</sup>, SCN<sup>-</sup>) were used to test the possibility of anion-induced polarization of the NH group. Cyanide (CN<sup>-</sup>) and hydroxide (OH<sup>-</sup>) were the only two anions that caused polarization of the NH group according to UV-vis and NMR spectra analysis. However, the red shift in the UV-vis spectra caused by CN<sup>-</sup>-induced polarization of the NH group was only 7 nm, and an observable color change was not evident. Metal ions, such as Ca<sup>2+</sup>, Cd<sup>2+</sup>, Co<sup>2+</sup>, Cu<sup>2+</sup>, Fe<sup>2+</sup>, Hg<sup>2+</sup>, Mg<sup>2+</sup>, Mn<sup>2+</sup>, Ni<sup>2+</sup> and Zn<sup>2+</sup>, were tested in binding studies. Chemosensors **1** and **2** underwent significant color change from orange to dark blue

Department of Applied Chemistry, National Chiao Tung University, Hsinchu, Taiwan, Republic of China. E-mail: spwu@mail.nctu.edu.tw; Fax: +886 3 5723764; Tel: +886 3 5712121-ext 56506

† Electronic supplementary information (ESI) available: <sup>1</sup>H NMR spectra of **1** and its mixture with CN<sup>-</sup> in chloroform, Job's plot of a 1 : 1 complex of **2**-Cu<sup>2+</sup>, Benesi-Hilderbrand plot of **2** with Cu(BF<sub>4</sub>)<sub>2</sub>, IR spectra of **1** and a 1/Cu(II) mixture in methanol, IR spectra of **1** and its mixture with Cu(II) in CH<sub>3</sub>CN, IR spectra of **1** and its mixture with Ni(II) in methanol. See DOI: 10.1039/b822613j

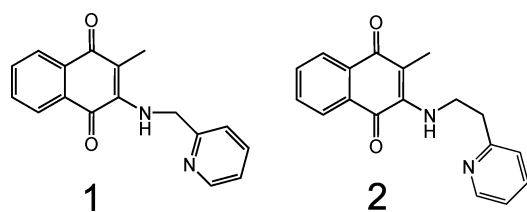


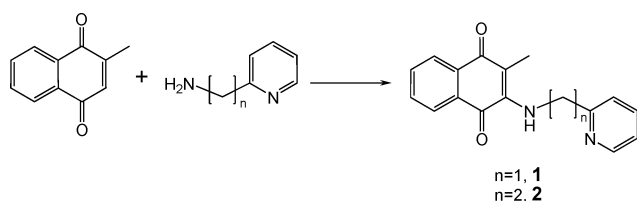
Fig. 1 Molecular structures of chemosensors **1** and **2**.

with a 168 nm red shift in the presence of  $\text{Cu}^{2+}$ . The pH titration experiments on  $\text{Cu}^{2+}$  binding with **1** and **2** revealed that the color change upon  $\text{Cu}^{2+}$  binding was mainly due to the deprotonation of the secondary amine attached to 2-methyl-1,4-naphthoquinone.

## Results and discussion

### Synthesis of chemosensor **1** and **2**

Chemosensors **1** and **2** were synthesized by direct nucleophilic addition of 2-(aminomethyl)pyridine and 2-(aminoethyl)pyridine to 2-methyl-1,4-naphthoquinone, respectively (Scheme 1). The reaction was under aerobic conditions, in which molecular oxygen was available to oxidize the intermediate aminoquinol, to allow the regeneration of the aminoquinone moiety in the final product.<sup>10</sup> Both compounds were purified by column chromatography (eluting with ethyl acetate–hexane in a 1 : 1 ratio) with yields of **1** and **2** being 60% and 55%, respectively.



Scheme 1 Synthesis of chemosensors **1** and **2**.

### Anion-induced polarization of the NH group in chemosensor **1** and **2**

The absorption band of chemosensor **1** was influenced by pH (Fig. 2). With decreasing pH (7.5 to 1), the maximum absorption wavelength shifted from 466 to 450 nm, *i.e.* a 16 nm blue-shift compared to neutral **1**. This was due to protonation of the amine group attached to 1,4-naphthoquinone under acidic conditions. At pH values above 7.5, the maximum absorption wavelength remained unchanged. The pH titration on chemosensor **2** had similar observation. The pH titration profile of chemosensor **2** was almost identical to that of chemosensor **1**. In order to test the possibility of anion-induced deprotonation of the NH group, several anions ( $\text{CN}^-$ ,  $\text{F}^-$ ,  $\text{Cl}^-$ ,  $\text{Br}^-$ ,  $\text{H}_2\text{PO}_4^-$ ,  $\text{HSO}_4^-$ ,  $\text{NO}_3^-$ ,  $\text{ClO}_4^-$ ,  $\text{CO}_3^{2-}$ ,  $\text{OH}^-$ ,  $\text{SCN}^-$ ) were mixed with **1** in a chloroform solution. Cyanide ( $\text{CN}^-$ ) and hydroxide ( $\text{OH}^-$ ) were the only two anions which caused polarization of the NH group according to NMR and UV-vis spectra analysis. In the NMR spectra of chemosensor **1**, the proton (NH) signal at 7.01 ppm almost completely disappeared upon the addition of  $\text{CN}^-$  or  $\text{OH}^-$  (see ESI).<sup>†</sup> Fig. 3 shows the UV-vis spectra of chemosensor **1** with

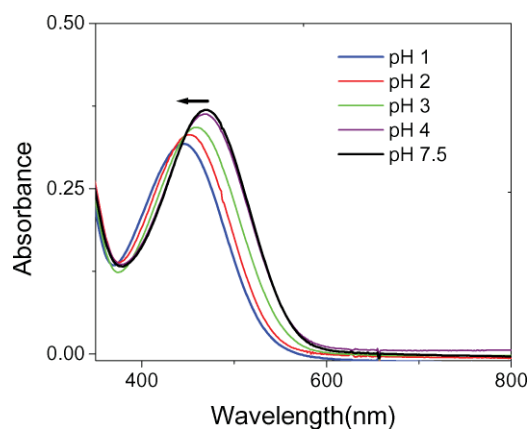


Fig. 2 Absorption spectra of **1** (100  $\mu\text{M}$ ) at pH 1 (blue), pH 2 (red), pH 3 (green), pH 4 (purple) and pH 7.5 (black) in the methanol–water (v/v = 4 : 1, 20 mM buffer) solution.

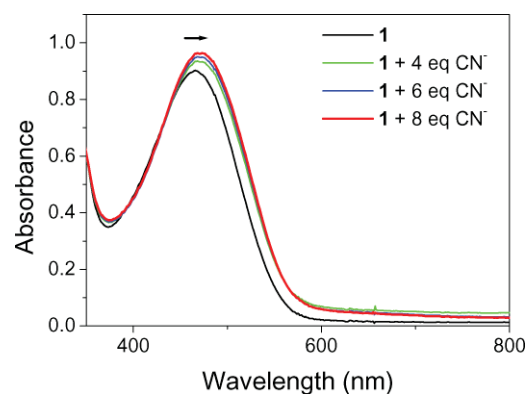


Fig. 3 Absorption spectra of **1** (250  $\mu\text{M}$ ) with different equivalent amounts of  $\text{CN}^-$  in chloroform.

the addition of varying concentrations of  $\text{CN}^-$ . The maximum absorption wavelength shifted from 466 to 473 nm upon  $\text{CN}^-$  addition.  $\text{CN}^-$ -induced polarization of the NH group in **1** only caused a 7 nm red shift, in which an observable color change was not evident. Similarly,  $\text{OH}^-$ -induced polarization of the NH group in **1** only caused a 6 nm red shift (from 466 to 472 nm). For chemosensor **2**, cyanide ( $\text{CN}^-$ ) and hydroxide ( $\text{OH}^-$ ) were also the only two anions which caused polarization of the NH group. The red shift caused by  $\text{CN}^-$  or  $\text{OH}^-$  induced polarization of the NH group in **2** was also small ( $\sim 7$  nm) and no obvious color change was observed.

### Spectrophotometric estimation of Cu(II) binding by **1** and **2**

The ability of **1** and **2** to form complexes with metal ions was studied using UV-vis spectroscopy. Transition metal ions, such as  $\text{Ca}^{2+}$ ,  $\text{Cd}^{2+}$ ,  $\text{Co}^{2+}$ ,  $\text{Cu}^{2+}$ ,  $\text{Fe}^{2+}$ ,  $\text{Hg}^{2+}$ ,  $\text{Mg}^{2+}$ ,  $\text{Mn}^{2+}$ ,  $\text{Ni}^{2+}$  and  $\text{Zn}^{2+}$  were tested using chemosensors **1** and **2** for metal ion detection.  $\text{Cu}^{2+}$  was the only ion that caused an observable color change from orange to dark blue for both chemosensors **1** and **2** (Fig. 4). Fig. 5 shows the absorption change during  $\text{Cu}^{2+}$  titration with chemosensor **1**. With increasing  $\text{Cu}^{2+}$  concentrations, the absorbance at 466 nm decreased and a new band centered at



**1**                      **1 + Cu<sup>2+</sup>**

**Fig. 4** The colors of chemosensor **1** (100  $\mu\text{M}$ ) and its mixture with  $\text{Cu}^{2+}$  (500  $\mu\text{M}$ ) in the methanol–water ( $v/v = 4 : 1$ , 20 mM Hepes buffer, pH 7.0) solution.

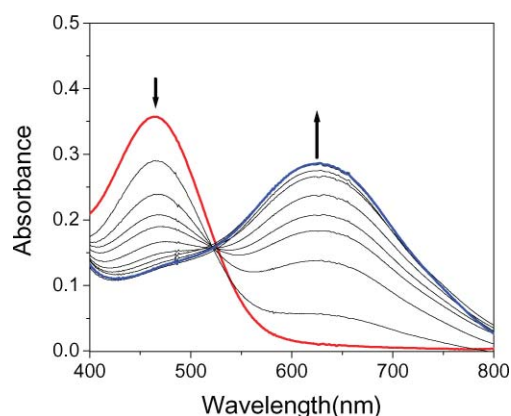


**Fig. 5** Absorption change in the UV/Vis spectra of **1** (red line, 100  $\mu\text{M}$ ) upon  $\text{Cu}(\text{BF}_4)_2$  titration in a methanol–water ( $v/v = 4/1$ , 20 mM Hepes buffer, pH 7.0) solution. The concentrations of  $\text{Cu}(\text{BF}_4)_2$  used are 50, 100, 150, 200, 250, 300, 350, 400, 450, 500  $\mu\text{M}$ .

634 nm was formed. This 168 nm red shift manifested itself as a visually observable color change from orange to dark blue. Fig. 6 shows the absorbance ratios ( $A_{634}/A_{466}$ ) of chemosensors **1** and **2** in the presence of different metal ions. For both chemosensor **1** and **2**,  $\text{Cu}^{2+}$  was the only ion with a high ratio ( $A_{634}/A_{466}$ ). Chemosensors **1** and **2** demonstrated highly selective detection for  $\text{Cu}^{2+}$ .

The pH effect on  $\text{Cu}^{2+}$  binding in both chemosensors **1** and **2** was studied using UV-vis spectroscopy (Fig. 7). A wavelength of 634 nm was used for monitoring the blue complexes. The absorbance at 634 nm suddenly increased at pH 6.0, and reached a maximum in the pH range of 6.0–7.5 for **1** and in the pH range of 6.0–7.0 for **2**. This indicates that the formation of blue **1**- $\text{Cu}^{2+}$  and **2**- $\text{Cu}^{2+}$  complexes is a deprotonation process. When the pH value was higher than 8, the absorbance at 634 nm gradually decreased. This is due to the dissociation of blue **1**- $\text{Cu}^{2+}$  and **2**- $\text{Cu}^{2+}$  complexes, which resulted in lower absorbance at 634 nm. For **1**, there was a flat area (absorbance of 0.1) in the pH range of 4–5.5. This indicated the formation of non-deprotonated **1**- $\text{Cu}^{2+}$  complexes. At pH < 4, the absorbance was close to zero. The **1**- $\text{Cu}^{2+}$  and **2**- $\text{Cu}^{2+}$  complexes did not exist in this pH range.

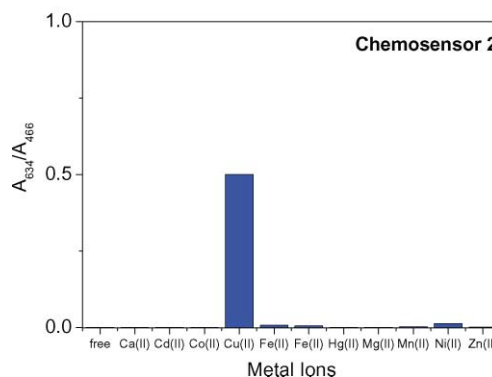
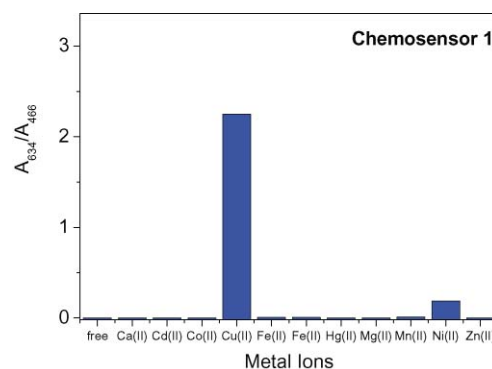


**Fig. 6** Spectrophotometric response of **1** (top) and **2** (bottom) with different metal ions. **1** or **2** ( $10^{-4}$  M) was mixed with metal ions ( $5 \times 10^{-4}$  M) in a methanol–water ( $v/v = 4 : 1$ , 20 mM Hepes buffer, pH 7.0) solution.

#### Stoichiometries and affinity constants of **1**- $\text{Cu}^{2+}$ and **2**- $\text{Cu}^{2+}$ complexes

The binding stoichiometry of **1**- $\text{Cu}^{2+}$  and **2**- $\text{Cu}^{2+}$  complexes was determined using Job's plot experiments.<sup>11</sup> In Fig. 8, the absorbance at 634 nm was plotted against the molar fraction of **1** or **2** under a constant total concentration. A maximum absorbance was reached when the molar fraction was 0.5. These results indicate a 1 : 1 ratio for both the **1**- $\text{Cu}^{2+}$  and **2**- $\text{Cu}^{2+}$  complexes. The association constant  $K_a$  was evaluated graphically by plotting  $1/\Delta A$  against  $1/[\text{Cu}^{2+}]$  (Fig. 9). The data was linearly fit according to the Benesi–Hilderbrand equation and the  $K_a$  value was obtained from the slope and intercept of the line.<sup>11</sup> The  $K_a$  values of **1**- $\text{Cu}^{2+}$  and **2**- $\text{Cu}^{2+}$  complexes were  $1.02 \pm 0.04 \times 10^4 \text{ M}^{-1}$  and  $8.50 \pm 0.18 \times 10^3 \text{ M}^{-1}$ , respectively. Chemosensor **1** had a slightly higher association constant than chemosensor **2**.

To gain a clearer understanding of the structure of **1**- $\text{Cu}^{2+}$  complexes, we used IR spectroscopy to obtain structural information about  $\text{Cu}^{2+}$  binding in **1**. The IR spectra were mainly characterized by the band in the carbonyl region ( $1672 \text{ cm}^{-1}$ ), which corresponds to a structural mode involving asymmetric stretching of the two carbonyl groups.<sup>12</sup> Binding of  $\text{Cu}^{2+}$  with **1** resulted in a shift from  $1672 \text{ cm}^{-1}$  to  $1664 \text{ cm}^{-1}$  (see Fig. S6 in the ESI).<sup>†</sup> This facilitated a direct interaction between  $\text{Cu}^{2+}$  and the C=O bond.<sup>13</sup> There was a bond formed between  $\text{Cu}^{2+}$  and the oxygen atom in the C=O bond. Chemosensor **1** behaves like a tridentate ligand, in which  $\text{Cu}^{2+}$  is bound with two nitrogen atoms and one oxygen atom in 1,4-naphthoquinone (Scheme 2). This model is consistent with

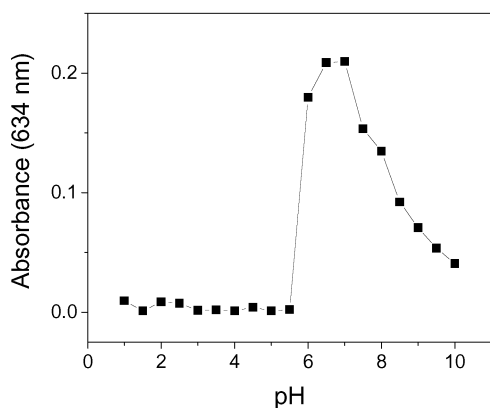
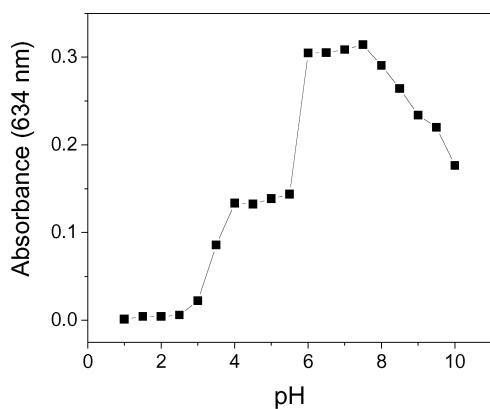


**Fig. 7** pH titration of Cu(II) binding with chemosensor **1** (top) and **2** (bottom). **1** or **2** ( $10^{-4}$  M) was mixed with metal ions ( $5 \times 10^{-4}$  M) in a methanol–water ( $v/v = 4 : 1$ , 20 mM buffer) solution.

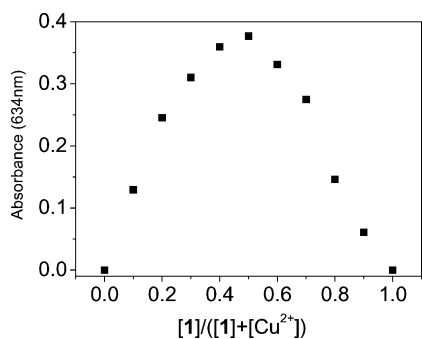


**Fig. 8** Job's plot of a 1 : 1 complex of **1**-Cu<sup>2+</sup>, where the absorbance at 634 nm was plotted against the mole fraction of Cu<sup>2+</sup> at a constant total concentration of  $2.0 \times 10^{-4}$  M in methanol.

previous results where Cu<sup>2+</sup> ions form a 1 : 1 ratio complex with chemosensor **1** and **2**.

#### Reversible color change observed by Cu<sup>2+</sup> binding with **1** in CH<sub>3</sub>CN

In order to study the solvent effect on Cu<sup>2+</sup> binding in both chemosensors **1** and **2**, acetonitrile (an aprotic solvent) was also used in the study. In CH<sub>3</sub>CN, the only color change was observed when Cu<sup>2+</sup> was mixed with chemosensor **1**. Mixing of chemosensor **2** with Cu<sup>2+</sup> did not result in obvious color change. Also, other metal ions did not cause any color change when mixing with both

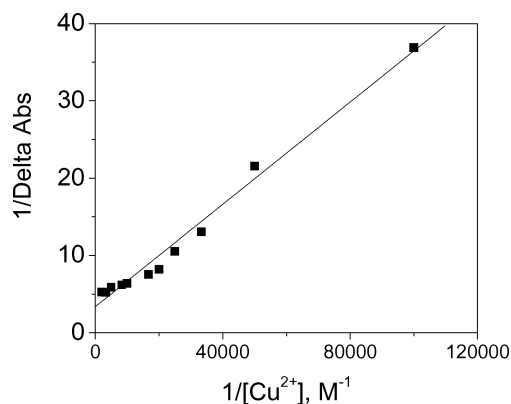
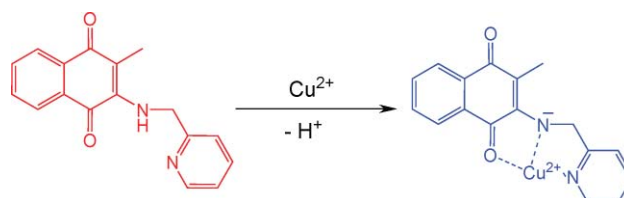


**Fig. 9** Benesi–Hilderbrand plot of **1** with Cu(BF<sub>4</sub>)<sub>2</sub>.



**Scheme 2** The bonding model of the **1**-Cu<sup>2+</sup> complex.

chemosensors **1** and **2**. Cu<sup>2+</sup> binding with **1** in CH<sub>3</sub>CN produced a reversible color change (orange–blue–orange). Upon mixing Cu<sup>2+</sup> with **1**, the color changed from orange to blue, but the color rapidly turned orange again. Fig. 10A shows the decay process of the blue **1**-Cu<sup>2+</sup> complexes. The absorption band centered at 634 nm was observed first, followed by a rapid decrease. The decay process was monitored using a wavelength of 634 nm and fit to a first order exponential decay with a one-minute half-life. The final maximum absorption was located at 455 nm, differing from the maximum absorption of metal-free **1** at 464 nm. This indicated the formation of the orange **1**-Cu<sup>2+</sup> complex. The reversible color change was mainly due to re-protonation in the secondary amine. The deprotonated **1**-Cu<sup>2+</sup> complex in CH<sub>3</sub>CN has a short half-life and is re-protonated quickly.

A reversible color change (orange–blue–orange) was also observed in the **1**-Ni<sup>2+</sup> complexes in methanol. In Fig. 10B, two absorption bands centered at 466 nm and 634 nm were observed upon mixing Ni<sup>2+</sup> with **1**. The first band at 466 nm was mainly the absorption of metal-free **1** and the second band at 635 nm was a new band, similar to the absorption band of the blue **1**-Cu<sup>2+</sup> complex. The decay process was monitored using a wavelength of 634 nm and fitted with a first-order exponential decay with a half-life of 45 min. The final maximum absorption was located at 480 nm with a higher absorbance compared to that of metal-free **1**. This indicated the formation of the orange **1**-Ni<sup>2+</sup> complex. Ni<sup>2+</sup> binding with **1** in methanol induced deprotonation of NH and formed a blue deprotonated **1**-Ni<sup>2+</sup> complex. Due to a short half-life, the deprotonated **1**-Ni<sup>2+</sup> complex rapidly re-protonated and the color changed back to orange.

The decay process of blue **1**-Cu<sup>2+</sup> complex was also investigated using IR spectroscopy. In CH<sub>3</sub>CN, addition of Cu<sup>2+</sup> with **1** resulted in a C=O band shift from 1674 cm<sup>-1</sup> to 1670 cm<sup>-1</sup> (see Fig. S7 in the ESI).† Compared to the C=O band shift (8 cm<sup>-1</sup>) of deprotonated **1**-Cu<sup>2+</sup> complexes, this 4 cm<sup>-1</sup> shift indicates weaker

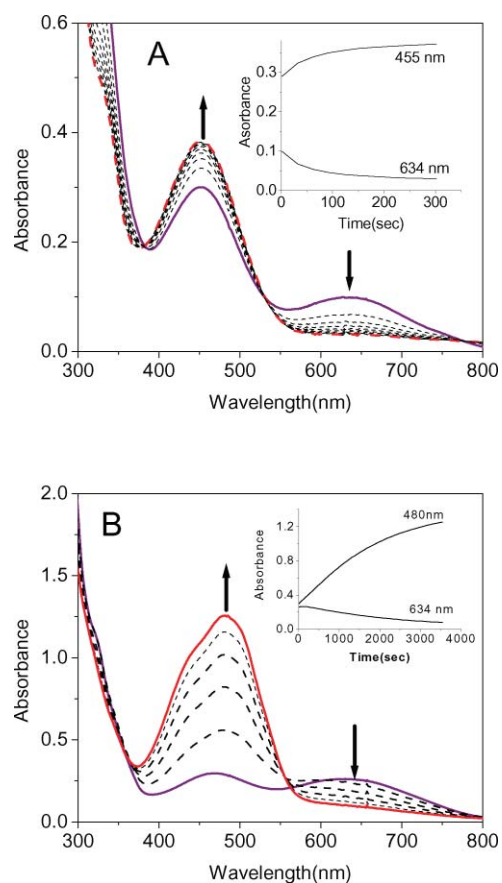


**Fig. 10** (A) Absorbance change in the UV-vis spectra of **1** with Cu(BF<sub>4</sub>)<sub>2</sub> in acetonitrile. The inset contains two time courses monitored at 634 nm and 455 nm, respectively. (B) Absorbance change in the UV-vis spectra of **1** with Ni(BF<sub>4</sub>)<sub>2</sub> in methanol. The inset contains two time courses monitored at 634 nm and 480 nm, respectively. The blue line represents the initial spectrum and the red line is the final spectrum. The concentrations of **1** and metal ions were 100  $\mu$ M.

interaction between Cu<sup>2+</sup> and the carbonyl oxygen in protonated **1**-Cu<sup>2+</sup> complexes. Cu<sup>2+</sup> binding with **1** caused deprotonation of NH and formed a bond with the carbonyl oxygen. The structure of deprotonated **1**-Cu<sup>2+</sup> complexes was planar (Scheme 2). In CH<sub>3</sub>CN, deprotonated **1**-Cu<sup>2+</sup> complexes were not stable and re-protonated quickly. In protonated **1**-Cu<sup>2+</sup> complexes, Cu<sup>2+</sup> binding with **1** was through the lone pair electrons in the NH group. This resulted in a twisted structure in which the interaction between Cu<sup>2+</sup> and the carbonyl oxygen was weak. For the **1**-Ni<sup>2+</sup> complex in methanol, the C=O absorption band was almost identical to that of metal-free **1**. This indicates that no bond formation occurred between Ni<sup>2+</sup> and the oxygen atom in C=O. Ni<sup>2+</sup> binding in **1** was mainly through two nitrogen atoms, differing from Cu<sup>2+</sup> binding in **1**.

## Conclusions

We have developed two 1,4-naphthoquinone based colorimetric chemosensors **1** and **2** for Cu<sup>2+</sup> detection. Chemosensors **1** and **2** function as tridentate ligands, which bind a Cu<sup>2+</sup> ion through three functional groups: amine nitrogen, pyridine nitrogen and quinone oxygen. The recognition of Cu<sup>2+</sup> ion by **1** and **2** gave rise

to color changes from orange to blue that was clearly observable to the naked eye. The color change was mainly due to Cu<sup>2+</sup> induced deprotonation of NH in **1** and **2**. Compared to the red shift (7 nm) caused by CN<sup>-</sup>-induced deprotonation of the NH group in **1**, the Cu<sup>2+</sup> induced deprotonation of NH in **1** and **2** had a larger red shift (168 nm). Cu<sup>2+</sup> not only induced deprotonation of NH in **1** and **2** upon binding but also affected the  $\pi$  to  $\pi^*$  transition which caused a significant red shift. A reversible color change (orange–blue–orange) was observed when chemosensor **1** was mixed with Cu<sup>2+</sup> in CH<sub>3</sub>CN. This represents a reversible process of deprotonation and re-protonation of **1**-Cu<sup>2+</sup> complexes, and also indicates a short half-life of the deprotonated **1**-Cu<sup>2+</sup> complexes in CH<sub>3</sub>CN.

## Experimental

### Materials and instrumentations

All solvents and reagents were obtained from commercial sources and used as received without further purification. UV-vis spectra were recorded on an Agilent 8453 UV-vis spectrometer. IR data were obtained on Bomem DA8.3 Fourier-transform infrared spectrometer. NMR spectra were obtained on a Bruker DRX-300 NMR spectrometer.

**Synthesis of chemosensors 1 and 2.** The reaction mixture containing 2-methyl-1,4-naphthoquinone (0.172 g, 1.00 mmol) and 2-(aminomethyl)pyridine (1.00 mmol) or 2-(aminoethyl)pyridine (1.00 mmol) in methanol was stirred for 12 h. The color changed from yellow to dark red. The solvent was removed by rotor vacuum and ethyl acetate was added to dissolve the reaction mixture. The product was separated in silica gel by eluting with ethyl acetate–hexane (1 : 1). A dark red band was collected and the yields of **1** and **2** were 60% and 55%, respectively, according to the amount of 2-methyl-1,4-naphthoquinone.

**Chemosensor 1.** EI-Mass  $m/z$  (%), 278 (31.5), 263 (28.6), 107 (12.8), 93 (100). HRMS (EI)  $m/z$  calcd for C<sub>17</sub>H<sub>14</sub>N<sub>2</sub>O<sub>2</sub>, 278.1055, found, 278.1060. <sup>1</sup>H-NMR (300 MHz, CDCl<sub>3</sub>)  $\delta$ /ppm: 8.64 (1H, d, 3.5 Hz), 8.12 (1H, d, 7.3 Hz), 8.05 (1H, d, 7.3 Hz), 7.68–7.76 (2H, m), 7.60 (1H, t, 4.2 Hz), 7.16–7.26 (2H, m), 7.01 (1H, br), 5.00 (2H, s), 2.23 (3H, s). <sup>13</sup>C-NMR (75.4 MHz, CDCl<sub>3</sub>)  $\delta$ /ppm: 183.8, 183.0, 156.9, 148.5, 146.5, 138.5, 134.6, 133.6, 132.3, 131.0, 126.5, 126.4, 123.3, 122.6, 114.4, 49.5, 11.2.

**Chemosensor 2.** EI-Mass  $m/z$  (%), 293 (M + H<sup>+</sup>, 25.1), 200 (27.1), 106 (74.9), 93 (100). HRMS (EI)  $m/z$  calcd for C<sub>18</sub>H<sub>16</sub>N<sub>2</sub>O<sub>2</sub>, 292.1212, found 292.1212. <sup>1</sup>H-NMR (300 MHz, CDCl<sub>3</sub>)  $\delta$ /ppm: 8.58 (1H, d, 3.9 Hz), 8.05 (1H, t, 7.5 Hz), 7.95 (1H, d, 7.3 Hz), 7.67–7.52 (3H, m), 7.19 (2H, d, 7.4 Hz), 6.23 (1H, br), 3.99 (2H, d, 6.5 Hz), 3.09 (2H, t, 6.4 Hz), 2.22 (3H, s). <sup>13</sup>C-NMR (75.4 MHz, CDCl<sub>3</sub>)  $\delta$ /ppm: 183.6, 182.7, 158.5, 149.4, 146.5, 137.3, 134.4, 133.6, 132.0, 130.6, 126.3, 126.1, 123.9, 122.2, 113.0, 45.0, 35.6, 11.3.

**Metal ion binding study by UV-vis spectroscopy.** Chemosensor **1** and **2** (10<sup>-4</sup> M) was added with different metal ions (5  $\times$  10<sup>-4</sup> M). All spectra were measured in 1.0 mL methanol–water solution ( $v/v = 4 : 1$ , 20 mM Hepes buffer, pH 7.0). The light path length of cuvette was 1.0 cm.

**The study of anion-induced polarization of chemosensor 1 and 2 using NMR and UV-vis spectroscopy.** Chemosensor **1** or **2** (2.5  $\times$  10<sup>-4</sup> M) was mixed with different tetrabutylammonium

anion salts (CN<sup>-</sup>, F<sup>-</sup>, Cl<sup>-</sup>, Br<sup>-</sup>, H<sub>2</sub>PO<sub>4</sub><sup>-</sup>, HSO<sub>4</sub><sup>-</sup>, NO<sub>3</sub><sup>-</sup>, ClO<sub>4</sub><sup>-</sup>, CO<sub>3</sub><sup>2-</sup>, OH<sup>-</sup>, SCN<sup>-</sup>, 1.0 × 10<sup>-3</sup> M). All spectra were measured in 1.0 mL chloroform and the light path length of cuvette was 1.0 cm.

**The pH dependence on Cu<sup>2+</sup> binding in chemosensor 1 and 2 studied by UV-vis spectroscopy.** Chemosensor **1** and **2** (10<sup>-4</sup> M) was added with Cu<sup>2+</sup> (5 × 10<sup>-4</sup> M) in 1.0 mL methanol–water solution (v/v = 4 : 1, 20 mM buffer). The buffers were: pH 1–2, KCl/HCl; pH 2.5–4, KHP/HCl; pH 4.5–6, KHP/NaOH; pH 6.5–10 Hepes.

**Determination of the binding stoichiometry and the stability constants K<sub>a</sub> of Cu(II) binding in chemosensor 1 and 2.** The binding stoichiometry of **1**-Cu<sup>2+</sup> and **2**-Cu<sup>2+</sup> complexes was determined by Job's plot experiments.<sup>11</sup> The absorbance at 634 nm was plotted against molar fraction of **1** or **2** under a constant total concentration. The concentration of the complex approached a maximum absorbance when the molar fraction was 0.5. These results indicate that both chemosensor **1** and **2** form a 1 : 1 complex with Cu<sup>2+</sup>. The stability constants K<sub>a</sub> of 1 : 1 **1**-Cu<sup>2+</sup> and **2**-Cu<sup>2+</sup> complexes were determined by the Benesi–Hilderbrand equation:<sup>11</sup>

$$1/\Delta A = 1/\Delta A_{\text{sat}} + 1/(\Delta A_{\text{sat}} K_a [\text{Cu}^{2+}]) \quad (1)$$

where  $\Delta A$  is the absorbance difference at 635 nm and  $\Delta A_{\text{sat}}$  is the maximum absorbance difference at 635 nm. The association constant K<sub>a</sub> was evaluated graphically by plotting 1/ΔA against 1/[Cu<sup>2+</sup>]. Typical plots (1/ΔA vs. 1/[Cu<sup>2+</sup>]) are shown in Fig. 3. Data were linearly fitted according to eqn (1) and the K<sub>a</sub> value was obtained from the slope and intercept of the line. The K<sub>a</sub> values of **1**-Cu<sup>2+</sup> and **2**-Cu<sup>2+</sup> complexes were 1.02 ± 0.04 × 10<sup>4</sup> M<sup>-1</sup> and 8.50 ± 0.18 × 10<sup>3</sup> M<sup>-1</sup>, respectively.

## Acknowledgements

We gratefully acknowledge the financial supports of the National Science Council (ROC) and National Chiao Tung University.

## Notes and references

- (a) R. Kramer, *Angew. Chem., Int. Ed.*, 1998, **37**, 772–773; (b) A. Torrado, G. K. Walkup and B. Imperiali, *J. Am. Chem. Soc.*, 1998, **120**, 609–610; (c) Y. Zheng, Q. Huo, P. Kele, F. M. Andreopoulos, S. M. Pham and R. M. Leblanc, *Org. Lett.*, 2001, **3**, 3277–3280; (d) Y. Zheng, K. M. Gattas-Asfura, V. Konka and R. M. Leblanc, *Chem. Commun.*, 2002, 2350–2351; (e) T. Gunnlaugsson, J. P. Leonard and N. S. Murray, *Org. Lett.*, 2004, **6**, 1557–1560; (f) L. Zeng, E. W. Miller, A. Pralle, E. Y. Isacoff and C. J. Chang, *J. Am. Chem. Soc.*, 2005, **128**, 10–11; (g) Z. Xu, X. Qian and J. Cui, *Org. Lett.*, 2005, **7**, 3029–3032; (h) X. Qi, E. J. Jun, L. Xu, S. Kim, J. S. J. Hong, Y. J. Yoon and J. Yoon, *J. Org. Chem.*, 2006, **71**, 2881–2884; (i) N. Kaur and S. Kumar, *J. Chem. Soc. Dalton Trans.*, 2006, 3766–3771; (j) N. Kaur and S. Kumar, *Chem. Commun.*, 2007, 3069–3070; (k) J. Liu and Y. Lu, *J. Am. Chem. Soc.*, 2007, **129**, 9838–9839.
- J. J. R. Frausto da Silva and R. J. P. Williams, *The Biological Chemistry of Elements: The Inorganic Chemistry of Life*, Clarendon Press, Oxford, 1993, pp. 388–397.
- J. A. Cowan, *Inorganic Biochemistry: An Introduction*, Wiley-VCH, New York, 1997, pp. 133–134.
- D. J. Waggoner, T. B. Bartnikas and J. D. Gitlin, *Neurobiol. Disease*, 1999, **6**, 221–230.
- C. Vulpe, B. Levinson, S. Whitney, S. Packman and J. Gitschier, *Nat. Genet.*, 1993, **3**, 7–13.
- P. C. Bull, G. R. Thomas, J. M. Rommens, J. R. Forbes and D. W. Cox, *Nat. Genet.*, 1993, **5**, 327–337.
- K. J. Barnham, C. L. Masters and A. I. Bush, *Nat. Rev. Drug Discov.*, 2004, **3**, 205–214.
- (a) T. Hayashita, T. Onodera, R. Kato, S. Nishizawa and N. Teramae, *Chem. Commun.*, 2000, 755–756; (b) J. L. Sessler and H. Miyaji, *Angew. Chem., Int. Ed.*, 2001, **40**, 154–157; (c) H. Miyaji, S. R. Collinson, I. Prokes and J. H. R. Tucker, *Chem. Commun.*, 2003, 64–65; (d) M. Boiocchi, L. D. Boca, D. E. Gomez, L. Fabbri, M. Licchelli and E. Monazani, *J. Am. Chem. Soc.*, 2004, **126**, 16507–16514; (e) D. E. Gomez, L. Fabbri, M. Licchelli, *J. Org. Chem.*, 2005, **70**, 5717–5720.
- L. Salmon-Chemin, E. Buisine, V. Yardley, S. Kohler, M. Debreu, V. Landry, C. Sergheraert, S. L. Craft, R. L. Krauth-Siegel and E. Davioud-Charvet, *J. Med. Chem.*, 2001, **44**, 548–565.
- M. Mure and J. P. Klinman, *J. Am. Chem. Soc.*, 1995, **117**, 8698–8706.
- T. Kao, C. Wang, Y. Pan, Y. Shiao, J. Yen, C. Shu, G. Lee, S. Peng and W. Chung, *J. Org. Chem.*, 2005, **70**, 2919–2920.
- J. Burie, C. Boullais, M. Nonella, C. Mioskowski, E. Nabedryk and J. Breton, *J. Phys. Chem. B*, 1997, **101**, 6607–6617.
- (a) G. Speier, J. Csihony, A. M. Whalen and C. G. Pierpont, *Inorg. Chim. Acta*, 1996, **245**, 1–5; (b) S. Roy, B. Sarkar, D. Bubrin, M. Niemeyer, S. Zalis, G. K. Lahiri and W. Kaim, *J. Am. Chem. Soc.*, 2008, **130**, 15230–15231.